Quantum Mechanical Studies of Residue-Specific Hydrophobic Interactions in p53−MDM2 Binding

Yun Ding,[†] Ye Mei,[†] and John Z. H. Zhang*[,†,‡]

Institute of Theoretical and Computational Chemistry, Key Laboratory of Mesoscopic Chemistry of Ministry of Education, School of Chemistry and Chemical Engineering, Nanjing University, Nanjing 210093, China, and Department of Chemistry, New York University, New York, New York 10003

Received: February 22, 2008; Revised Manuscript Received: May 5, 2008

Quantum chemistry calculations at the levels of MP2/cc-pVDZ and MP2/cc-PVTZ have been carried out to study residue-specific interactions at the hydrophobic p53−MDM2 binding interface. The result of the calculation, based on structures from nanosecond molecular dynamics simulation, revealed that ^{19}Phe, ^{22}Leu, and ^{23}Trp of p53 have the strongest binding interaction with MDM2 followed by ^{26}Leu and ^{27}Pro. The specific residues of MDM2 that have dominant binding interactions with p53 are specifically identified to be ^{51}Lys, ^{54}Leu, ^{62}Met, ^{67}Tyr, ^{72}Gln, ^{94}Lys, ^{96}His, and ^{100}Tyr. The p53−MDM2 binding interaction is dominated by van der Waals interaction and to a lesser degree by electrostatic interaction. The MP2 results are in generally good agreement with those from the force field calculation while the DFT/B3LYP calculation failed to give attractive interaction energies for certain residue−residue interactions due to the lack of dispersion energy.

I. Introduction

The p53 is an important tumor suppressor protein in regulating cell cycle arrest, apoptosis, and DNA repair.[1−3] In reality, over half of the human cancer is caused by mutations or deletions of alleles in p53.[4] In some of the remaining cancer cases, wild-type p53 is inactivated by the binding of the N-terminal domain of MDM2 oncoprotein to its transactivation domain.[5−8] The MDM2 oncoprotein is first found as the second of three amplified genes on marine double minute chromosomes.[9] The overexpression of MDM2 is found in many cancers, such as soft tissue sarcomas,[8] breast cancer,[10] etc., and it is believed that the separation of p53−MDM2 can reactivate the regulation of p53. Thus, inhibition of the p53−MDM2 binding is an important strategy for anticancer drug design.[11−13]

The X-ray crystal structure of p53−MDM2 binding complex (PDB ID: 1YCR; see Figure 1)[6] reveals that the short amphipathic α-helix formed by the 17−29 residues of p53 binds to the hydrophobic cleft of MDM2. The side chains of three hydrophobic residues, ^{19}Phe, ^{23}Trp, and ^{26}Leu, insert deeply into the hydrophobic cleft of MDM2 and contact tightly with the pocket.[6] The interaction between p53 and MDM2 mainly depends on the van der Waals interaction and is augmented by two hydrogen bonds. One of these two H-bonds is formed by the backbone NH in ^{19}Phe of p53 to the side chain of ^{72}Gln of MDM2. The other is formed by the indole ring of P53−^{23}Trp to the backbone CO of ^{54}Leu in MDM2. Therefor, ^{19}Phe and ^{23}Trp should be important residues to consider in the drug design. In fact, many drug candidates are designed to mimic the side chains of ^{19}Phe, ^{23}Trp, and ^{26}Leu of p53.[6] Recently, a fourth residue, ^{22}Leu was brought into attention and is believed to play an important role in the interaction with MDM2.[14] The designed compounds based on these four residues show high binding affinity.[14] In Figure 1, we also see that the aromatic ring of ^{27}Pro parallels the benzene ring of ^{100}Tyr. This may also contribute to the binding of p53 to MDM2 and will be studied by quantum calculation.

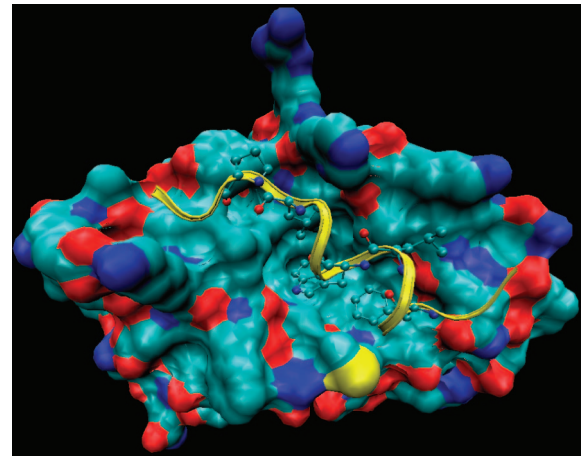

Figure 1. MDM2 is shown as VDW surface: cyan, carbon; blue, nitrogen; red, oxygen; yellow, sulfur. p53 (residue 17−29) is shown as yellow ribbon. ^{19}Phe, ^{22}Leu, ^{23}Trp, ^{26}Leu, and ^{27}Pro are shown in the CPK model.

The crystal structure of the protein complex provides the most important starting point for qualitative understanding of the binding mechanism. However, in order to gain a more quantitative description of the binding interaction, which is especially important for designing new effective inhibitors, it is desirable to carry out theoretical calculations to investigate protein−ligand interaction dynamics in detail. Although classical force field provides a convenient means to extract these information and for performing MD simulations, there are also known deficiencies in the standard force such as the lack of electronic polarization and multibody interactions involving delocalized electrons often present in the interaction involving aromatic rings. Thus, it is highly desirable if one can also perform quantum chemisty calculations at appropriate levels for protein interaction. Comparison between force field and quantum

* Corresponding author. E-mail: john.zhang@nyu.edu.
† Nanjing University.
‡ New York University.

10.1021/jp8015886 CCC: $40.75
Published on Web 08/16/2008

chemistry calculations should enable us to reach more conclusive results in quantitative understanding of the protein−ligand interaction. However, direct quantum chemistry calculation for a protein system is not practical due to the large size of the protein. Recently, fragment-based approaches[15−18] have been developed which makes quantum chemistry calculation for protein systems possible.

Since p53−MDM2 binding is believed to be dominated by van der Waals (vdW) interactions, quantum chemistry methods such as Hartree−Fock (HF) and density functional theory (DFT) are deficient in this respect because they are incapable of providing vdW or dispersion energies. In order to obtain vdW energies, post-Hartree−Fock methods such as Møller−Plesset (MP) perturbation and coupled cluster (CC) theories are often employed for this type of calculations.[19,20] Since CC calculation with large basis set is computationally impractical for large systems, MP2 calculation is often a preferred choice for computing practical systems to obtain correlation and dispersion energies with reasonable amount of computational cost.

In this paper, we employ fragment-based quantum chemistry approach and force field method in combination with molecular dynamics simulation to investigate residue-specific interactions in p53−MDM2 binding interface. To avoid confusions in notation, we denote residues in p53 by its sequence number and type, and those in MDM2 with an additional prime.

II. Computational Approach

A. Molecular Dynamics Simulation. The initial structure of p53−MDM2 was taken from the Protein Data Bank (PDB ID: 1YCR, see Figure 1). Hydrogen atoms are added using the leap module of Amber 9.[21] This complex was then soaked in a TIP3P water box with 10 Å buffer. Three chloride ions were added to neutralize the system. A 10 000-step minimization was carried out with a quadratic constraint on all 85 residues of MDM2 with force constant $k = 500$ kcal mol $^{-1}$ Å^{-2}, followed by a 30 100-step minimization without any restraints. The whole system was heated up to 300 K in 20 ps with a weak restraint force constant $k = 10$ kcal mol $^{-1}$ Å $^{-2}$ on MDM2. Finally, a 1 ns simulation with a time step of 2 fs was carried out at 300 K. All minimization and MD simulation were performed using Amber9. SHAKE[22] was used to constrain all chemical bonds containing hydrogen atoms. For long-range electrostatic interactions, the particle mesh Ewald (PME) method[23] is used, and a typical 10 Å cutoff is used for the van der Waals interactions. Langevin dynamics is applied to control the temperature with a collision frequency of 1.0 ps^{-1}. Configurations were collected every 0.2 ps.

B. Quantum Chemistry Calculation. Direct application of quantum chemistry methods to the entire p53−MDM2 complex is practically impossible in view of the present computational abilities. In addition, since we are interested in specific residue−residue interactions, it is desirable to employ fragment-based approaches to calculate interaction energies between individual residues. Among the molecular fragment approaches,[15−17] the MFCC method comes handy when computing reside-specific interaction energies.[17,18,24,25] When applying MFCC method to the p53−MDM2 system, both p53 and MDM2 are cut at peptide bonds and partitioned into amino acid based fragments with proper caps to saturate the chemical bonds.[17] The conjugate caps were used to mimic the adjacent amino acids. In this paper, we used the simplest cap, $CH_3CO-NHCH_3$, without side chain and the interaction energy in each p53−MDM2 residue pair can be calculated with minimal influence of the caps.

C. MM and QM Calculations. For five residues in p53, i.e., ^{19}Phe, ^{22}Leu, ^{23}Trp, ^{26}Leu, ^{27}Pro, Amber force field is first applied to calculate the interaction energy between individual residue pairs of p53 and MDM2. For those residue pairs whose interaction energies are more attractive than −2 kcal/mol, QM calculations for the involved residue pairs are further carried out. Residues are capped with $CH_3CO-NHCH_3$ according to the MFCC scheme. As is known, MP2 calculation of vdW energy converges slowly with the basis set and the computational cost scales as N^5 with the number of basis N.

In order to speed up the convergence in MP2 calculation, we introduce the middle bond function (MBF) to add to the standard cc-pvdZ basis set.[26−28] A previous study demonstrated that by including additional MBF, the MP2 energies at cc-pvdZ for benzene−benzene interactions are much improved and are closer to those calculated at cc-pvtZ.[29] The added MBF are denoted as {6s6p4d2f} and are added at the middle point between the centers of p53 and MDM2 residue pairs. The position of the middle point is defined by the equation

$$(\text{middle bond position})_{ij} = \frac{1}{2}\left(\sum_{k=1}^{N_i}\frac{\vec{r}_{ik}}{N_i} + \sum_{k=1}^{N_j}\frac{\vec{R}_{jk}}{N_j}\right) \qquad (1)$$

in which N_i and N_j represent the number of atoms in the ith fragment of p53 and jth fragment of MDM2, respectively. The $\vec{r}_{ik}$ and $\vec{R}_{jk}$ are the coordinates of the kth atoms in the ith fragment of p53 and the jth fragment of MDM2. The exponents of these midbond functions are (0.05, 0.10, 0.20, 0.40, 0.80, 1.60) for s and p functions, (0.05, 0.15, 0.45, 1.35) for d functions, and (0.2, 0.6) for f functions.[29] Previous studies indicated that MBF is efficient for weakly bonded systems.[26−29]

III. Results and Discussion

A. Force Field Result. After two steps of minimization, followed by 20 ps of heating, a 1 ns isothermal−isobaric MD is run. Conformations and the corresponding energy information were collected every 0.2 ps and a total of 5100 snapshots were collected for analysis. The time evolution of root-mean-square deviations (rmsd) is shown in Figure 2. The upper curve represents the rmsd of all the atoms in p53 (residue 17−29), which fluctuates around 1.8 Å. The lower curve represents the rmsd of backbone atoms, i.e., C_α, C, and N atoms in p53 and MDM2. It fluctuates around 0.8 Å. All the rmsd was compared to the initial structure. The time evolution of the total energy is shown in Figure 3. Three configurations, marked with circles in Figure 3, were extracted from the trajectory for the MM and QM analysis and labeled as C1, C2, and C3 in the following discussions.

The Amber 03 force field[32,33] was used for the interaction energy calculation. Only nonbonded interactions are involved as given in eq 2.

$$\Delta E = \sum\left(\frac{A_{ij}}{R_{ij}^{12}} - \frac{B_{ij}}{R_{ij}^{6}}\right) + \sum\frac{q_i q_j}{R_{ij}} \qquad (2)$$

Here, the first sum represents the van der Waals interaction energy and the second sum is the electrostatic interaction energy. Figure 4 shows the MM interaction energy of the five residues in p53 to each residue in MDM2 (residue 25−109) in the three snapshots, respectively. Due to the hydrophobicity of the binding interface, there are only short-range interactions, and the majority of residue−residue interactions are negligible. The total interaction energies of ^{19}Phe, ^{22}Leu, ^{23}Trp, ^{26}Leu, and ^{27}Pro in p53 to MDM2 are listed in Table 1.

Among the interactions, ^{19}Phe and ^{23}Trp of p53 have the strongest binding interaction with MDM2. The total interaction energies of ^{19}Phe are −21.209, −24.580, and −24.024 kcal/

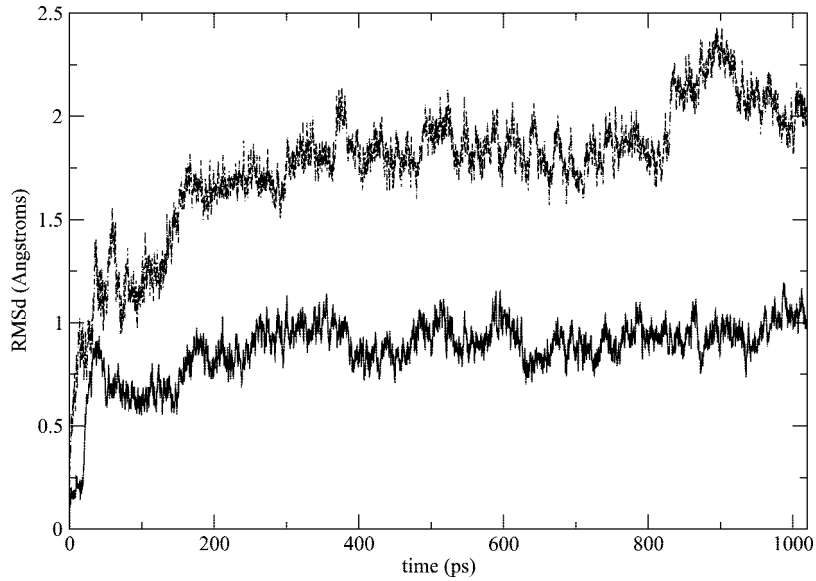

Figure 2. Time evolution of root-mean-square deviation (rmsd). The gray dashed line represents the rmsd of all the atoms in p53 (residue 17−29). The black solid line represents the rmsd of backbone atoms, i.e., C_α, C and N, in p53 and MDM2 (residue 25−109).

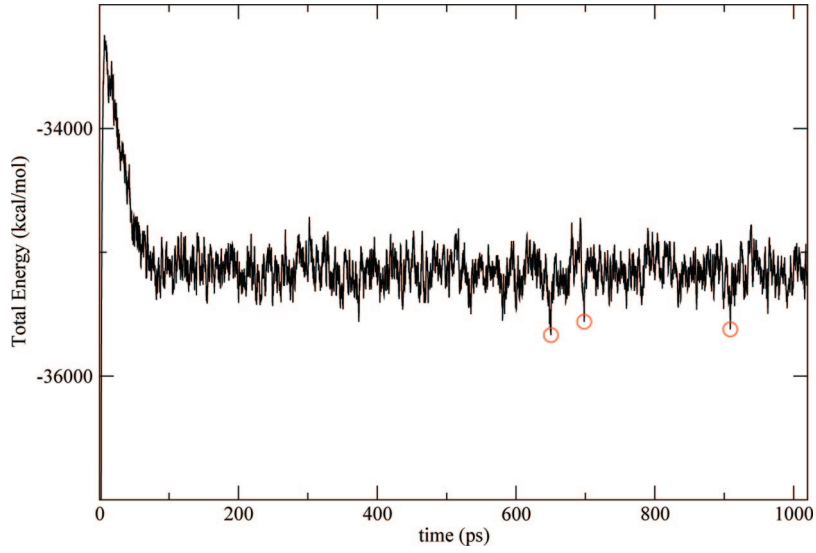

Figure 3. Time evolution of total energy in MD. The red circles represent the three chosen configurations, C1, C2, and C3, consecutively.

mol in C1, C2, and C3, respectively. The corresponding interactions with ^{23}Trp are −23.523, −23.089, and −17.498 kcal/mol. These strong interactions are dominated by hydrogen bonding as well as vdW interactions. In comparison to these two residues, the interaction of ^{22}Leu with MDM2 is weaker, and the total interaction energy is in the range of −12.6 to −15.4 kcal/mol. The interactions of ^{26}Leu and ^{27}Pro to MDM2 are even weaker, which are both under −8.2 kcal/mol. However, these residues may still be very important for p53/MDM2 binding. Judging by the strength of the interaction energy, ^{22}Leu should be more important in binding to MDM2 than ^{26}Leu, although the side chain of ^{26}Leu inserts more deeply into MDM2. The residue pairs with strong interaction energies in all three configurations are listed in Table 2 for reference. Further study at QM level on these residue pairs are discussed in the next section.

However, it is important to keep in mind that the listed MM interaction energies can only be used as a reference when considering the actual contribution to binding. Because, in addition to the gas-phase interaction energy, there are also the effects of solvation and entropy. Thus, one should not take the quantitative values of these interaction energies too seriously. Rather, these interaction energies can be used as a basis to understand the molecular mechanism of binding by identifying specific residues responsible for binding interaction.

B. QM Calculation. We next performed quantum chemistry calculations to investigate detailed residue-specific interactions in the binding interface of p53−MDM2 complex. All the quantum calculations were performed with Gaussian 03,[30] and results are listed in Table 2. Calculations are done for three chosen configurations with the lowest local energies. These three configurations are labeled as C1, C2, and C3 as denoted in Figure 3. Since high-level quantum chemistry calculation for all the residue−residue interactions in p53−MDM2 complex is computationally expensive and not necessary, we only choose those residue pairs whose interaction energies from the force field calculation are larger than a certain threshold limit.

For the strong interacting pairs selected from the force field calculation, we performed quantum calculations at the level of MP2/cc-pVDZ. In view of the nature of slow convergence with basis size, we also performed calculation at MP2/cc-pVDZ-6s6p4d2f by adding MBF functions. This can give us a

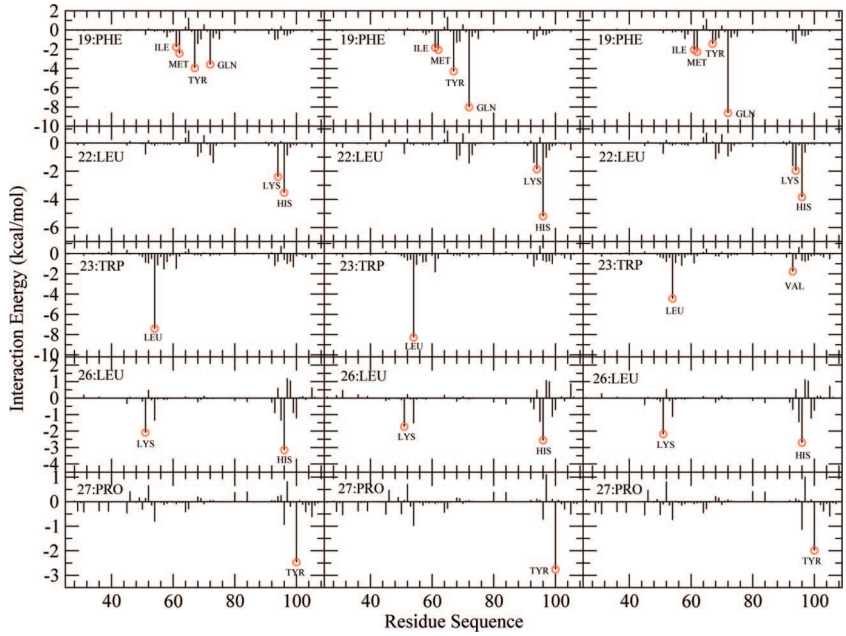

Figure 4. Interaction energy spectra at MM level for five residues in p53: ^{19}Phe, ^{22}Leu, ^{23}Trp, ^{26}Leu, and ^{27}Pro in three configurations. The left column is for C1, the middle column is for C2, and the right column is for C3.

TABLE 1: Total Interaction Energies for p53 Residues Binding with MDM2 from Force Field Calculation (kcal/mol)

		interaction energy (kcal/mol)		
SEQ	RES	C1	C2	C3
19	PHE	−21.209	−24.580	−24.024
22	LEU	−12.600	−15.438	−12.902
23	TRP	−23.523	−23.089	−17.493
26	LEU	−8.131	−6.567	−7.358
27	PRO	−5.202	−5.501	−5.481

reasonable estimate on the possible error due to incomplete basis size in MP2 calculation. If the difference between two sets of calculation is small, the error is expected to be small. As is discussed elsewhere,[26−29] adding MBF can give much improved energies without much additional computational cost over the corresponding standard basis set calculations. For consistency, the counterpoise correction method of Boys and Bernardi[31] is used in all the calculations to correct basis set superposition error. In these calculations, each residue was capped with the smallest conjugate caps—CH_3CO−$NHCH_3$—without side chains. So the contribution from the conjugate caps in the calculated residue−residue interaction energy is minimal.

To estimate the contribution of caps to the calculated interaction energy, we also calculated the interaction energies between ^{19}Phe and the concap between ^{61}Ile′ and ^{62}Met′ in C2 and C3 at MP2/cc-pVDZ level. The calculations give, respectively, −0.272 and −0.341 kcal/mol, which is relatively small compared to the binding energy of ^{19}Phe to ^{61}Ile′ and ^{62}Met′. Thus, the contribution to the calculated interaction energy from ^{61}Cap is negligible and the interaction energies are mainly originated from the residues themselves.

The quantum result for residue−residue interaction energies in Table 2 shows that the energies obtained from the standard MP2/cc-pVDZ calculation are quite consistent with those from the augmented MBF calculation of MP2/cc-pVDZ-6s6p4d2f. To be more specific, the interaction energies from the augmented MP2/cc-pVDZ-6s6p4d2f calculations are slightly larger than from the corresponding MP2/cc-pVDZ calculations. This is an indication that the basis size cc-pVDZ is quite decent and close to the convergence. Obviously, the energies from the MP2/cc-pVDZ-6s6p4d2f should be more accurate.[29] The exception is seen for ^{26}Leu−^{96}His′ pair for which the interacting energies from the MP2/cc-pVDZ-6s6p4d2f calculation are significantly larger than those of MP2/cc-pVDZ. This will be discussed further below.

The calculated quantum results are quite consistent and in good agreement with those from the corresponding force field calculation as shown in Table 2. The ^{26}Leu−^{96}His′ interaction is an exception where the quantum result is sensitive to the size of basis sets used. The corresponding interaction energy from the standard MP2/cc-pVDZ calculation is much smaller than that from the force field as shown in Table 2. However, with the addition of MBF 6s6p4d2f in basis set, the calculated interaction energy clearly increases (by a factor of 6 in C2). Further calculation at larger MP2/cc-pVTZ level give further improved energies that are quite consistent with the force field energies with the largest difference being only 0.43 kcal/mol in C2. The energy decomposition at MM level shows that the ^{26}Leu−^{96}His′ interaction is mainly from the van der Waals contribution and the electrostatic interaction is negligible. In order to obtain more vdW energy in MP2 calculation, larger basis set is needed and this explains the above result.

As a further demonstration, we also performed DFT calculations at B3LYP/cc-pVDZ and B3LYP/cc-pVTZ for three selected residue pairs, i.e., ^{19}Phe−^{67}Tyr′, ^{22}Leu−^{96}His′, and ^{26}Leu−^{96}His′. Energy decomposition in Table 2 shows that in both ^{19}Phe−^{67}Tyr′ and ^{26}Leu−^{96}His′ the interactions are mainly due to van der Waals energy with little contribution from the electrostatic interaction. Thus, it is not surprising to see that DFT calculations give essentially repulsive energies for these residue pairs since DFT is incapable of giving vdW energy as shown clearly in Table 3.

Quantum calculation shows that ^{19}Phe, ^{22}Leu, and ^{23}Trp have the largest contributions to interaction. In particular, ^{19}Phe has multiple strong interactions with MDM2 residues including ^{62}Met′, ^{67}Tyr′, and ^{72}Gln′. The ^{22}Leu mainly interacts with ^{94}Lys′ and ^{96}His′. Also, residue ^{23}Trp is hydrogen-bonded to ^{54}Leu′ and interacts weakly with other residues.

TABLE 2: Quantum Calculation of Interaction Energies for Five p53 Residues Binding to Specific MDM2 Residues (kcal/mol)

		QM interaction energy (MP2)			MM interaction energy (Amber FF03)		
p53	MDM2	VDZ[a]	VDZ*[b]	VTZ[c]	FF03[d]	E_{vdW}[e]	E_{ele}[f]
				C1			
^{19}Phe	^{62}Met	−2.700	−3.451		−2.442	−1.780	−0.662
	^{67}Tyr	−3.462	−4.678		−3.949	−3.777	−0.172
	^{72}Gln	−4.228	−5.215		−3.597	−1.914	−1.683
^{22}Leu	^{94}Lys	−3.050	−3.704		−2.400	−2.480	0.080
	^{96}His	−4.398	−4.856		−3.535	−1.777	−1.758
^{23}Trp	^{54}Leu	−7.097	−7.937		−7.417	−1.696	−5.721
^{26}Leu	^{51}Lys	−1.423	−1.584		−2.101	−0.065	−2.036
	^{96}His	−0.747	−2.037	−2.960	−3.155	−3.365	0.210
^{27}Pro	^{100}Tyr	−2.368	−2.992		−2.474	−1.628	−0.846
				C2			
^{19}Phe	^{61}Ile	−1.078	−1.534		−1.840	−1.785	−0.055
	^{61}Cap	−0.272					
	^{62}Met	−2.500	−3.114		−2.064	−1.598	−0.466
	^{67}Tyr	−3.483	−4.952		−4.307	−4.345	0.038
	^{72}Gln	−7.850	−8.904		−8.025	−2.685	−5.340
^{22}Leu	^{94}Lys	−1.197	−1.921		−1.861	−2.356	0.495
	^{96}His	−6.297	−7.042		−5.212	−1.855	−3.357
^{23}Trp	^{54}Leu	−8.327	−8.950		−8.288	−2.842	−5.446
^{26}Leu	^{51}Lys	−1.151	−1.268		−1.741	−0.045	−1.696
	^{96}His	−0.209	−1.272	−2.138	−2.572	−2.725	0.153
^{27}Pro	^{100}Tyr	−2.184	−2.569		−2.762	−1.754	−1.008
				C3			
^{19}Phe	^{61}Ile	−1.311	−1.895		−2.052	−2.001	−0.051
	^{61}Cap	−0.341					
	^{62}Met	−2.095	−3.221		−2.276	−1.459	−0.817
	^{67}Tyr	−1.563	−1.927		−1.438	−1.332	−0.106
	^{72}Gln	−8.387	−9.953		−8.635	−2.825	−5.810
^{22}Leu	^{94}Lys	−2.956	−3.931		−1.962	−2.788	0.826
	^{96}His	−5.142	−5.659		−3.847	−1.733	−2.114
^{23}Trp	^{54}Leu	−4.188	−4.827		−4.438	−2.306	−2.132
	^{93}Val	−0.802	−1.219		−1.762	−2.226	0.464
^{26}Leu	^{51}Lys	−1.416	−1.586		−2.192	−0.054	−2.138
	^{96}His	−0.905	−2.229	−2.888	−2.718	−2.219	−0.499
^{27}Pro	^{100}Tyr	−1.557	−1.873		−1.990	−1.408	−0.582

[a] VDZ refers to cc-pVDZ basis set. [b] VDZ* refers to cc-pVDZ basis set with the bond function 6s6p4d2f. [c] VTZ refers to cc-pVTZ. [d] Interaction energies calculated from force field 03 in Amber 9. [e] E_{vdW} refers to the van der Waals interaction in force field. [f] E_{ele} refers to the MM electrostatic interaction.

TABLE 3: Calculated Interaction Energies (in kcal/mol) of p53 Residues Binding to MDM2 Residues at B3LYP Level

p53−MDM2	basis	C1	C2	C3
^{19}Phe−^{67}Tyr	cc-pVDZ	1.661	2.399	−0.179
	cc-pVTZ	1.482	2.163	−0.189
^{22}Leu−^{96}His	cc-pVDZ	−3.037	−5.095	−3.991
	cc-pVTZ	−3.085	−5.131	−3.959
^{26}Leu−^{96}His	cc-pVDZ	4.689	4.331	3.772
	cc-pVTZ	4.635	4.375	3.777

IV. Conclusion

In this work, we carried out molecular mechanics and quantum chemistry calculations to investigate residue-specific interactions in p53/MDM2 binding. Both calculations show that ^{19}Phe, ^{22}Leu, and ^{23}Trp have the largest contribution to binding interaction to MDM2, followed by ^{26}Leu and ^{27}Pro. ^{26}Leu is also an important residue in P53/MDM2 binding, and including this interaction may help in the design of new inhibitors to MDM2. The p53−MDM2 binding interaction is dominated by van der Waals interaction augmented by additional hydrogen bondings. The current study shows that correlated quantum chemistry methods such as MP2 with large basis sets are necessary in order to obtain correct residue-specific hydrophobic interaction energies in protein−protein binding interface. The density functional methods are inappropriate in the computation of these weak binding interactions because they missed van der Waals interaction in p53−MDM2 binding.

The results from the current MP2 calculation are in general agreement with the AMBER force field. This underscores the importance of dispersion energy in the p53−MDM2 interaction. The current study also demonstrates that it is realistic to employ MP2 or even higher ab initio methods such as coupled cluster methods to obtain more accurate interaction energy for protein−protein interaction. This is especially encouraging since through explicit comparison between force field and high-level quantum chemistry calculations, it is possible to improve the force field parameters to make them more accurate for describing protein−protein interactions.

Acknowledgment. This work is partially supported by the National Science Foundation of China (grant No. 20773060) and National Basic Research Program of China (grant No. 2004CB719901).

References and Notes

(1) Levine, A. J. *Cell* **1997**, *88*, 323.
(2) Vogelstein, B.; Lane, D.; Levine, A. J. *Nature* **2000**, *408*, 307.
(3) Wu, X.; Bayle, J. H.; Olson, D.; Levien, A. J. *Genes Dev.* **1993**, *7*, 1126.
(4) Hollstein, M.; Sidransky, D.; Vogelstein, B.; Harris, C. C. *Science* **1991**, *253*, 49.
(5) Momand, J.; Zambetti, G. P.; Olson, D. C.; George, D.; Levine, A. J. *Cell* **1992**, *69*, 1237.
(6) Kussie, P. H.; Gorina, S.; Marechal, V.; Elenbaas, B.; Moreau, J.; Levine, A. J.; Pavletich, N. P. *Science* **1996**, *274*, 948.
(7) Lane, D. P.; Hall, P. A. *Trends Biochem. Sci.* **1997**, *22*, 372.
(8) Oliner, J. D.; Kinzler, K. W.; Meltzer, P. S.; George, D. L.; Vogelstein, B. *Nature* **1992**, *358*, 80.
(9) Cahilly-Snyder, L.; Yang-Feng, T.; Francke, U.; George, D. L. *Somatic Cell Mol. Genet.* **1987**, *13*, 235.
(10) Kumar, S. K.; Hager, E.; Pettit, C.; Gurulingappa, H.; Davidson, N. E.; Khan, S. R. *J. Med. Chem.* **2003**, *46*, 2813.
(11) Chene, P. *Nat. Rev. Cancer* **2003**, *3*, 102.
(12) Kritzer, J. A.; Lear, J. D.; Hodsdon, M. E.; Schepartz, A. J. *Am. Chem. Soc.* **2004**, *126*, 9468.
(13) Galatin, P. S.; Abraham, D. J. *J. Med. Chem.* **2004**, *47*, 4163.
(14) Ding, K.; Lu, Y.; Nicolovska-Coleska, Z.; Wang, G.; Qiu, S.; Shangary, S.; Gao, W.; Qin, D.; Stuckey, J.; Krajewski, K.; Roller, P. P.; Wang, S. *J. Med. Chem.* **2006**, *49*, 3432.
(15) Kitaura, K.; Ikeo, E.; Asada, T.; Nakano, T.; Uebayasi, M. *Chem. Phys. Lett.* **1999**, *313*, 701.
(16) Nakano, T.; Kaminuma, T.; Sato, T.; Akiyama, Y.; Uebayasi, M.; Kitaura, K. *Chem. Phys. Lett.* **2000**, *318*, 614.
(17) Zhang, D. W.; Zhang, J. Z. H. *J. Chem. Phys.* **2003**, *119*, 3599.
(18) Zhang, D. W.; Zhang, J. Z. H. *J. Theor. Comput. Chem.* **2004**, *3*, 43–49.
(19) Li, A. H.; Chao, S. C. *J. Chem. Phys.* **2006**, *125*, 094312.
(20) Zhechkov, L.; Heine, T.; Patchkovskii, S.; Seifert, G.; Duarte, H. A. *J. Chem. Theory Comput.* **2005**, *1*, 841.
(21) Case, D. A.; Darden, T. A.; Cheatham, T.E. III,; Simmerling, C. L.; Wang, J.; Duke, R. E.; Luo, R.; Merz, K. M.; Pearlman, D. A.; Crowley, M.; Walker, R. C.; Zhang, W.; Wang, B.; Hayik, S.; Roitberg, A.; Seabra, G.; Wong, K. F.; Paesani, F.; Wu, X.; Brozell, S.; Tsui, V.; Gohlke, H.; Yang, L.; Tan, C.; Mongan, J.; Hornak, V.; Cui, G.; Beroza, P.; Mathews, D. H.; Schafmeister, C.; Ross, W. S.; Kollman, P. A. *AMBER 9*; University of California: San Francisco, 2006.
(22) Ryckaert, J.-P.; Ciccotti, G.; Berendsen, H. J. C. *J. Comput. Phys.* **1977**, *23*, 327.
(23) Darden, T.; York, D.; Pedersen, L. *J. Chem. Phys.* **1993**, *98*, 10089.
(24) Zhang, D. W.; Xiang, Yun.; John, Z. H. *J. Phys. Chem. B* **2003**, *107*, 12039.
(25) He, X.; Mei, Y.; Xiang, Y.; Zhang, D. W.; Zhang, J. Z. H. *Proteins: Struct., Funct. Bioinformatics* **2005**, *61*, 423–432.
(26) Tao, F. M.; Pan, Y. K. *J. Phys. Chem.* **1991**, *95*, 3582.
(27) Tao, F. M.; Pan, Y. K. *J. Chem. Phys.* **1992**, *97*, 4989.
(28) Tao, F. M. *Int. Rev. Phy. Chem.* **2001**, *20*, 617.

(29) Ding, Y.; Mei, Y.; Zhang, J. Z. H.; Tao, F. M. *J. Comput. Chem.* **2008**, *29*, 275.

(30) Frisch, M. J.; Trucks, G. W.; Schlegel, H. B.; Scuseria, G. E.; Robb, M. A.; Cheeseman, J. R.; Montgomery, J. A., Jr.; Vreven, T.; Kudin, K. N.; Burant, J. C.; Millam, J. M.; Iyengar, S. S.; Tomasi, J.; Barone, V.; Mennucci, B.; Cossi, M.; Scalmani, G.; Rega, N.; Petersson, G. A.; Nakatsuji, H.; Hada, M.; Ehara, M.; Toyota, K.; Fukuda, R.; Hasegawa, J.; Ishida, M.; Nakajima, T.; Honda, Y.; Kitao, O.; Nakai, H.; Klene, M.; Li, X.; Knox, J. E.; Hratchian, H. P.; Cross, J. B.; Bakken, V.; Adamo, C.; Jaramillo, J.; Gomperts, R.; Stratmann, R. E.; Yazyev, O.; Austin, A. J.; Cammi, R.; Pomelli, C.; Ochterski, J. W.; Ayala, P. Y.; Morokuma, K.; Voth, G. A.; Salvador, P.; Dannenberg, J. J.; Zakrzewski, V. G.; Dapprich, S.; Daniels, A. D.; Strain, M. C.; Farkas, O.; Malick, D. K.; Rabuck, A. D.; Raghavachari, K.; Foresman, J. B.; Ortiz, J. V.; Cui, Q.; Baboul, A. G.; Clifford, S.; Cioslowski, J.; Stefanov, B. B.; Liu, G.; Liashenko, A.; Piskorz, P.; Komaromi, I.; Martin, R. L.; Fox, D. J.; Keith, T.; Al-Laham, M. A.; Peng, C. Y.; Nanayakkara, A.; Challacombe, M.; Gill, P. M. W.; Johnson, B.; Chen, W.; Wong, M. W.; Gonzalez, C.; Pople, J. A. *Gaussian 03, Revision D.01*; Gaussian, Inc.: Wallingford, CT, 2004.

(31) Boys, S. F.; Bernardi, F. *Mol. Phys.* **1970**, *19*, 553.

(32) Duan, Y.; Wu, C.; Chowdhury, S.; Lee, M. C.; Xiong, G.; Zhang, W.; Yang, R.; Cieplak, P.; Luo, R.; Lee, T. *J. Comput. Chem.* **2003**, *24*, 1999.

(33) Lee, M. C.; Duan, Y. *Proteins* **2004**, *55*, 620.

JP8015886